Study of the compatibility of 3D-printed loads with a space environment

13-16 October 2026
ESA/ESTEC, Noordwijk, The Netherlands

Lana Damaj[(1)], Azar Maalouf[(1)], Thierry Abadie[(2)], Jessica Benedicto[(1)], Alexis Chevalier[(1)], Juan-Antonio Duran Venegas[(2)], Yann Cailloce[(2)], Kevin Elis[(3)], Vincent Laur[(1)],

[(1)]Lab-STICC/UBO
Lab-STICC (UMR6285), 6 av, Victor Le Gorgeu - CS93837
29238 Brest, France
Email: lana.damaj@univ-brest.fr , azar.maalouf@univ-brest.fr , jessica.benedicto@univ-brest.fr , alexis.chevalier@univ-brest.fr , vincent.laur@univ-brest.fr

[(2)]Thales Alenia Space
26 avenue J.F. Champollion, BP 33787_31037 Toulouse, France
Email: thierry.abadie@thalesaleniaspace.com , yann.cailloce@thalesaleniaspace.com , juan-antonio.duran-venegas@thalesaleniaspace.com

[(3)] Centre National d'Etudes Spatiales (CNES), Toulouse 31401, France
Email: Kevin.Elis@cnes.fr

INTRODUCTION

Matched waveguide terminations (loads) are essential passive components in microwave systems because they suppress reflections at the end of transmission paths, thereby preserving signal integrity. They are widely used to terminate unused ports in passive microwave devices, such as hybrid couplers, and to prevent undesired reflections. Similarly, loads are often added to configure a circulator as an isolator. In rectangular waveguide technology, matched terminations are generally realized as short-circuited waveguide sections loaded with a lossy absorbing material. As the electromagnetic wave propagates through the absorber, its energy is progressively converted into heat [1]. Although this approach provides excellent broadband matching, it often results in bulky and relatively heavy components, limiting their integration into compact Radio-Frequency (RF) front ends [2].

Additive manufacturing has emerged as a promising alternative by enabling the fabrication of lightweight and geometrically complex structures while reducing material consumption and production cost [3], [4]. Among the various additive manufacturing techniques, fused deposition modelling (FDM) has attracted particular interest because it offers significant design freedom [5], enabling the realization of graded, tapered [6], and multi-material [7] absorber geometries that are difficult or impossible to fabricate using conventional techniques such as machining and molding. However, the design of waveguide terminations remains a challenging multi-objective optimization problem, requiring a compromise between impedance matching, compactness, thermal performance, power handling, reproducibility, and cost. Thermoplastic-based 3D-printing technologies offer new topological possibilities to optimize this trade-off. However, conventional 3D-printing thermoplastics are generally not compatible with the thermal and mechanical requirements of space applications [8]. Consequently, the development of space-compatible printable materials has become a key challenge for the deployment of additively manufactured microwave components in aerospace applications.

In this study, three high-temperature thermoplastic composites are investigated to evaluate their suitability for the fabrication of space-compatible rectangular waveguide loads. The first material, denoted Ice9 Aero, is a polyetherketoneketone (PEKK)-based composite supplied by TCPoly. The other two materials, commercially available from 3DXTECH, are electrostatic discharge (ESD) grades consisting of either a PEKK or PEEK matrix filled with multiwall carbon nanotubes. These materials combine the high thermal stability and the electrical losses introduced by the conductive fillers, making them promising candidates for space-compatible microwave absorbers.

In this work, the dielectric properties of three high-temperature conductive thermoplastic composites are first characterized over a broad frequency and temperature range. These materials are then used to design and optimize 3D-printed rectangular waveguide loads through a comprehensive comparison of eighteen absorber topologies for Ku-band operation. The most promising designs are fabricated and experimentally validated in terms of microwave performance, reproducibility, and power-handling capability under both ambient and representative space environmental conditions. Finally, the selected topology is extended to Ka-band operation and evaluated under vacuum and high-temperature

conditions. The results demonstrate the potential of high-temperature 3D-printed thermoplastic composites for the realization of lightweight, space-compatible waveguide terminations.

MATERIAL SELECTION AND CHARACTERIZATION

As introduced previously, the additive manufacturing process considered in this work is fused deposition modeling (FDM). This technique builds 3D components by selectively depositing successive layers of molten polymer or polymer-matrix composite [9], [10]. The raw material is supplied as a filament, which is driven by a motor into a heated extrusion nozzle and deposited onto the build platform following a predefined toolpath. After each layer is completed, the build platform moves vertically to enable the deposition of the next layer.

Since the objective of this work is to design and fabricate rectangular waveguide loads with high power-handling capability, the selected materials must combine high thermal stability with sufficiently high dielectric losses. Three conductive high-temperature thermoplastic composites were therefore investigated in terms of both their microwave dielectric properties and printability: Ice9 Aero, PEKK-ESD, and PEEK-ESD. A comparison of their main characteristics is provided in Table 1.

Table 1. Comparison of material properties provided by the suppliers

Material	From	Thermal conductivity ($W.m^{-1}.K^{-1}$)	Glass transition temperature (T_g °C)	Melting point (T_m °C)	Resistivity (Ω.m)
Ice9 Aero	TCPoly	3	-	-	-
PEKK-ESD	3DXTECH	0.25	162	305	107 to 109
PEEK-ESD	3DXTECH	0.25	143	343	107 to 109

The three materials were printed using a 3NTR A2v4 printer. Prior to fabrication, the printing parameters were optimized for the selected materials. Because Ice9 Aero, PEKK-ESD, and PEEK-ESD exhibit similar thermomechanical properties, the same processing conditions were adopted for all three. The printer is equipped with a nozzle 0.4 mm in diameter, an extrusion temperature of 390 °C, a build plate temperature of 110 °C, and a chamber temperature of 75 °C. A layer thickness of 0.2 mm, a printing speed of 30 mm/s, and 100% infill with a concentric perimeter and 90° cross-hatched pattern were employed. ABS was used as a support material to improve adhesion to the build plate and was subsequently removed by dissolution in acetone. The printed parts were then dried in an oven at 65 °C for at least 12 h.

Several sets of samples were manufactured for electromagnetic and thermal characterization. Samples were fabricated by FDM and printed under the same conditions as the final waveguide loads, since the dielectric properties are known to depend on the printing parameters [11]. Waveguide samples compatible with WR-90, WR-62, and WR-42 standards were fabricated for X (8-12 GHz), Ku (12-18 GHz), and Ka-band (18-26.5 GHz) dielectric measurements, respectively. Additional samples were produced for free-space and coaxial dielectric characterization up to 40 GHz, as well as for thermal conductivity measurements. The dielectric properties of the selected materials were characterized using several measurement techniques. Rectangular waveguide measurements were performed in the X-band and Ku-band, together with APC7 coaxial line measurements over the 0.05–18 GHz frequency range. The complex permittivity (ε'-jε") was extracted from measured S-parameters by a standard Nicolson-Ross-Weir algorithm [12], [13].

Fig. 1 illustrates the frequency dependence of the dielectric properties up to 18 GHz. All three materials exhibit dispersive behavior, with PEEK-ESD showing the strongest variation over the investigated frequency range.

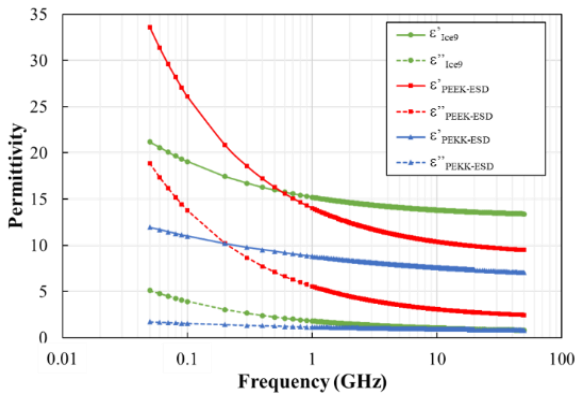


Fig. 1. Dielectric properties of Ice9 Aero, PEEK-ESD and PEKK-ESD in the 0,05-18 GHz frequency band

A comparison of the dielectric characteristics of the three materials in Ku-band is summarized in Table 2.

Table 2. Comparison of dielectric characteristics of materials in the Ku-band

Material	Permittivity	Loss tangent
Ice9 Aero	13.8	0.08
PEKK-ESD	7.6	0.12
PEEK-ESD	10.4	0.3

The dielectric properties of the three materials were also characterized over the temperature range from −50°C to +100°C. Their thermal stability is an important parameter for high-power applications, as the absorber temperature increases when it is exposed to high incident power. The measurements were carried out using a coaxial line. To ensure accurate results, the empty sample holder was first characterized over the same temperature range to account for changes in conductivity and thermal expansion of the measurement fixture. Overall, the dielectric properties of the three materials remained relatively stable over the investigated temperature range. The permittivity of Ice9 Aero and PEKK-ESD varied by less than 5% between −50°C and +100°C, while that of PEEK-ESD showed a maximum variation below 10%. Fig. 2 illustrates the variation in the permittivity of PEEK-ESD as a function of temperature at 6 GHz.

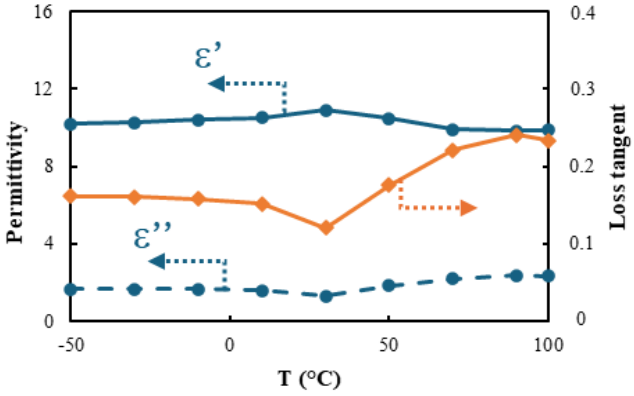


Fig. 2. Temperature dependence of ε′, ε″, and tan δ of PEEK-ESD at 6 GHz from −50 °C to +100 °C.

DESIGN OF 3D-PRINTED KU-BAND WAVEGUIDE LOADS

Various waveguide load topologies were designed and analyzed using CST Microwave Studio®. The designs targeted the Ku-band downlink of satellite communication systems (10.7–13.75 GHz), leading to the selection of the standard WR75 rectangular waveguide (19.05 mm × 9.525 mm). All topologies were evaluated in terms of reflection performance, compactness, and power-handling capability to identify the most suitable configurations for experimental validation.

Design Methodology and selected designs

Initially, the lengths of the loads were optimized to achieve a reflection level (|S11|) of less than -20 dB. Three parameters were compared: Power Loss Density (PLD), length, and volume of the loads. In order to simulate the absorption level, the load is backed by a metallic plate as shown in Fig.3

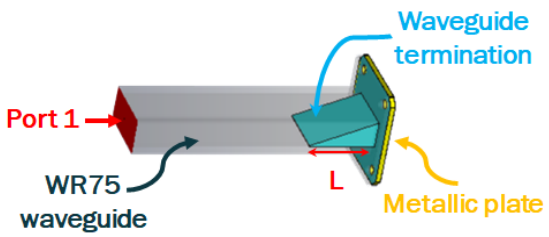
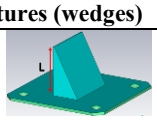
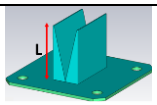
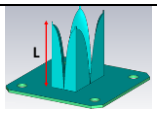
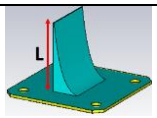


Fig. 3. Simulation setup of waveguide loads

Table 3 summarizes the simulated characteristics of some of the designed waveguide loads, including their length, maximum power loss density (PLD), and volume. The results show that the single- and double-linear wedges, as well as the exponential tetrahedral wedge, exhibit the most promising performance.

The single- and double (or dual) -wedge designs are the most compact when fabricated with PEEK-ESD. In addition, the double-linear wedge designed with PEKK-ESD provides the lowest maximum PLD, although its length is approximately three times greater than that of the corresponding PEEK-ESD design. The exponential tetrahedral wedge also achieves the smallest volume, and therefore the lowest weight, when fabricated with PEEK-ESD. Based on these results, the single-linear wedge, double-linear wedge, and exponential tetrahedral wedge were selected for fabrication by FDM using the three investigated materials.

Table 3. Comparison between simulated results of waveguide terminations with different shapes and materials.

Structures (wedges)	Materials	Length L(mm)	PLD (W/m^3)*10^5	Volume (mm^3)
 **Single linear**	Ice9 Aero	41	9.08	5267
	PEKK-ESD	**19**	40.39	3187
	PEEK-ESD	32	10.82	4417
 **Double linear**	Ice9 Aero	45	11.98	5817
	PEKK-ESD	**19**	14.17	3260
	PEEK-ESD	58	**6.31**	7095
 **Tetrahedral exponential**	Ice9 Aero	33	14.85	3202
	PEKK-ESD	23	14.15	**2618**
	PEEK-ESD	70	6.72	5616
 **Concave exponential**	Ice9 Aero	59	26.08	4172
	PEKK-ESD	25	44.09	2742
	PEEK-ESD	59	14.37	4172

Fabrication and low power experimental validation

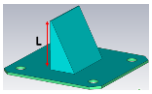
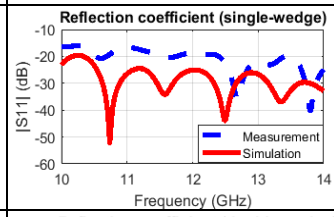
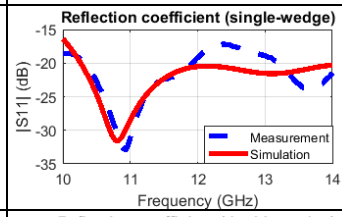
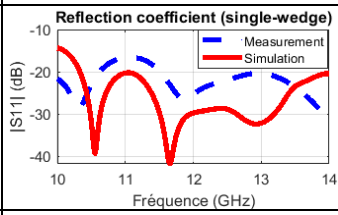
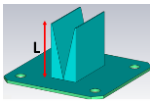
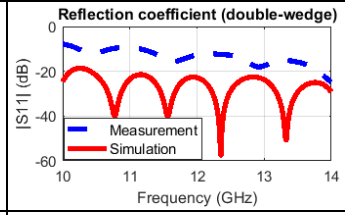
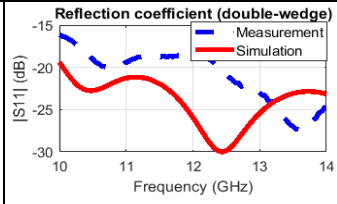
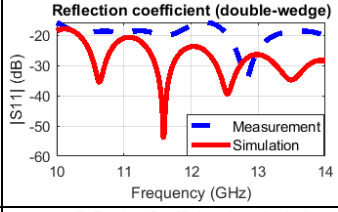
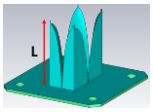
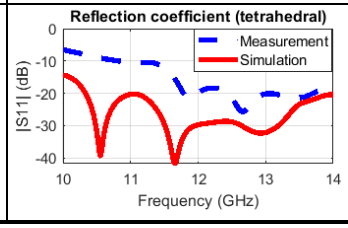
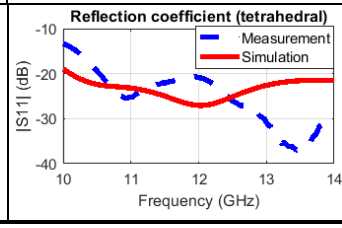
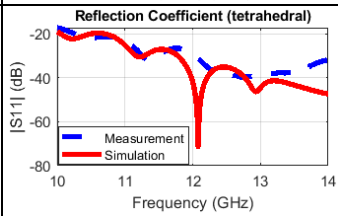
The selected waveguide loads were fabricated by FDM using PEEK-ESD, PEKK-ESD, and Ice9 Aero to evaluate their microwave performance. The reflection coefficient was measured using an R&S ZNB20 vector network analyzer with a low incident power level of −10 dBm. During the measurements, the device under test was inserted into a standard WR75 metallic waveguide and positioned against the metallic short-circuit plate closing the waveguide.

Table 4 compares the simulated and measured reflection coefficients of the three waveguide load topologies fabricated with the three investigated materials. Good agreement between simulations and measurements is observed for the single-linear wedge fabricated from PEEK-ESD and the exponential tetrahedral wedge fabricated from PEKK-ESD. In contrast, the Ice9 Aero-based loads exhibit significantly higher measured reflection levels than predicted by simulation. For the double-linear and exponential tetrahedral wedges fabricated from PEEK-ESD, slight deformation occurred during handling, leading to a small degradation in performance, although the overall agreement between simulations and measurements remained satisfactory. Likewise, the single- and double-linear wedges fabricated from PEKK-ESD showed good agreement between simulated and measured results.

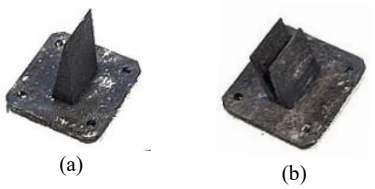
Since loads fabricated from Ice9 Aero and PEKK-ESD require volumes—and therefore masses—1.22 to 2.18 times greater than those fabricated from PEEK-ESD, and because Ice9 Aero exhibited a significant discrepancy between simulated and measured reflection levels, these two materials were not considered for further investigation. In addition, the handling difficulties encountered with the exponential tetrahedral wedge led to the selection of only the single- and double-linear wedge topologies fabricated from PEEK-ESD for subsequent power-handling experiments.

The measured reflection coefficients of these selected loads were slightly higher than the simulated values, mainly due to uncertainties in the dielectric properties of the material and manufacturing tolerances. To compensate for these discrepancies and ensure a measured reflection level below −20 dB over the 10.7–13.75 GHz frequency band, the designs were slightly optimized. The length of the single-linear wedge was increased to 33 mm, while that of the double-linear wedge was increased to 28 mm, yielding simulated reflection levels below −25 dB across the operating band.

Table 4. Simulated and measured reflection coefficients of the fabricated loads with the three materials.

Structures (wedges)	Ic9	PEEK-ESD	PEKK-ESD
 Linear			
 Dual linear			
 Tetrahedral exponential			

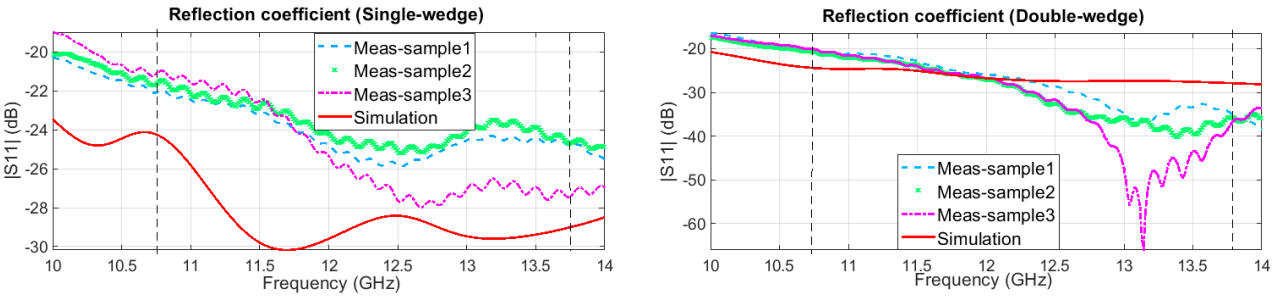
Finally, three identical samples of each topology were 3D-printed using PEEK-ESD to assess the reproducibility of the manufacturing process and the measured microwave performance (Fig. 4).



(a) (b)

Fig. 4. 3D-printing waveguide loads (a) single linear wedge and (b) double linear wedge

Fig. 5(a) and 5(b) show good agreement between the simulated and measured reflection coefficients. In both cases, the measured reflection level remains below −20 dB over the entire specified frequency band.



(a) (b)

Fig. 5. Simulated and measured reflection coefficient for single (a) and double (b) linear wedges

The power-handling capability of the two selected waveguide loads was evaluated at 11 GHz (room temperature and ground level pressure) using a dedicated high-power measurement setup. Fig. 6 shows the reflected power P_r as a function of the incident power P_{in} for both topologies. For the single-linear wedge, the relationship between P_r and P_{in} remains linear up to an incident power of 9.8 W, beyond which a deviation from linearity is observed. In contrast, the double-linear wedge maintains a linear response up to a higher incident power of 13.3 W before exhibiting the same

behaviour. These results indicate that the double-linear wedge provides a higher power-handling capability than the single-linear wedge, most likely because its larger interaction surface distributes the absorbed power more effectively.

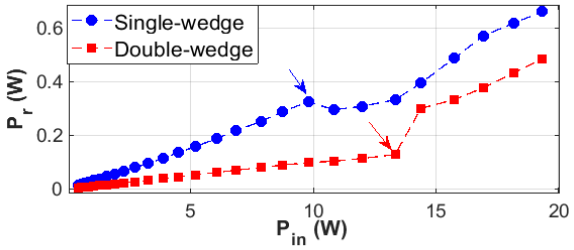
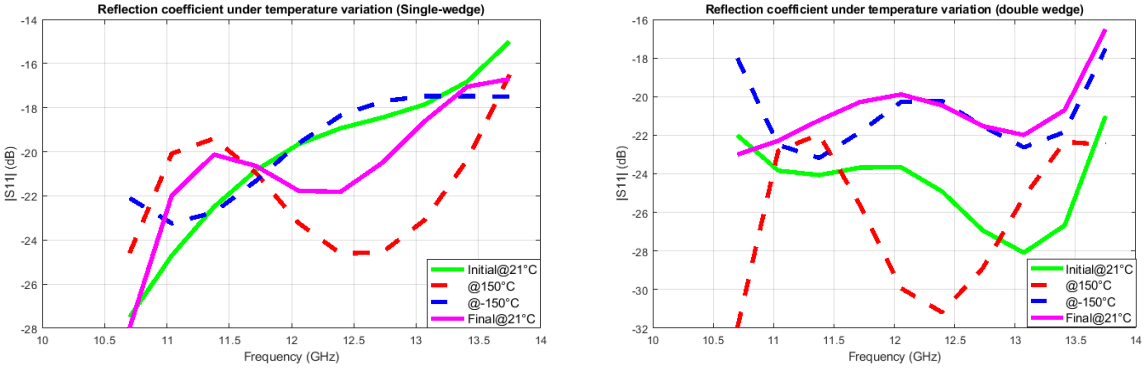


Fig. 6. Measurements of reflected power with respect to the incident power at 11 GHz for single and double linear wedges

Experimental validation in a space-like environment: vacuum and thermal testing

High-power tests under representative space environmental conditions were performed on each waveguide load (single- and double-linear wedges) at an incident power of 5 W (37 dBm). In addition, the variation of the reflection coefficient with temperature was measured over the range from −150°C to +150°C.

The reflection coefficient of each waveguide load was continuously monitored during a thermal cycle from −150°C to +150°C using a vector network analyzer. The measurements were performed in a thermal vacuum chamber under representative space environmental conditions. The chamber has a volume of 2 m³, an operating temperature range from −150°C to +150°C, and a temperature accuracy of ±1.5°C. During the tests, the pressure was maintained below 5×10^{-5} mbar. The reflection coefficient was measured over the frequency range from 10.5 to 14.0 GHz, corresponding to the Ku-band, while the temperature was varied between −150°C and +150°C. The temperature ramp rate was maintained below 2°C/min throughout the thermal cycle to ensure stable testing conditions.



(a) (b)

Fig. 7. Measured reflection coefficient for single (a) and double (b) linear wedges under temperature variation

Fig. 7 compares the reflection coefficient of the single-linear wedge measured before and after the thermal cycle, as well as at the extreme temperatures of −150°C and +150°C. The results show that the reflection coefficient remains at an acceptable level throughout the entire temperature range. For the double-linear wedge, the reflection coefficient also remains satisfactory, staying below −20 dB over most of the operating band. A slight degradation is observed at the upper end of the band, where the reflection coefficient increases to approximately −15 dB at −150°C and remains at a similar level after the load returns to room temperature (21°C). Despite this increase, the matching performance remains acceptable for the intended application.
This indicates that thermal cycling does not significantly degrade the electromagnetic performance of the load (|S11|<-15dB). This demonstrates good thermal stability and suggests that no permanent degradation occurred during the temperature test.

The high-power performance of the waveguide loads was evaluated under representative space environmental conditions after the temperature test. A continuous-wave RF signal at 12.2 GHz was applied to each load while it was placed inside a thermal vacuum chamber. The incident power was gradually increased from 0 W to 5 W in 0.5 W increments. During the test, the reflection coefficient and the temperature of the load were continuously monitored and recorded. The measurements were carried out in a thermal vacuum chamber with a volume of 2 m³, operating at a pressure below 5×10^{-5} mbar. The chamber maintained an ambient temperature of +150°C with a temperature accuracy of ±1.5°C throughout the experiment. The test was performed at the frequency of 12.2 GHz, corresponding to the center

of the Ku-band operating range, with the incident power increased in 0.5 W steps from 0 W to 5 W. The chamber temperature was kept constant at +150°C during the entire measurement.

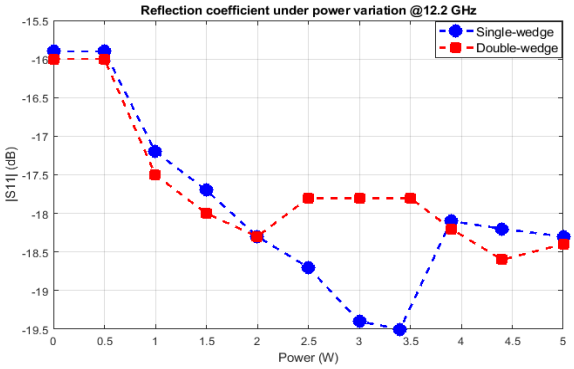


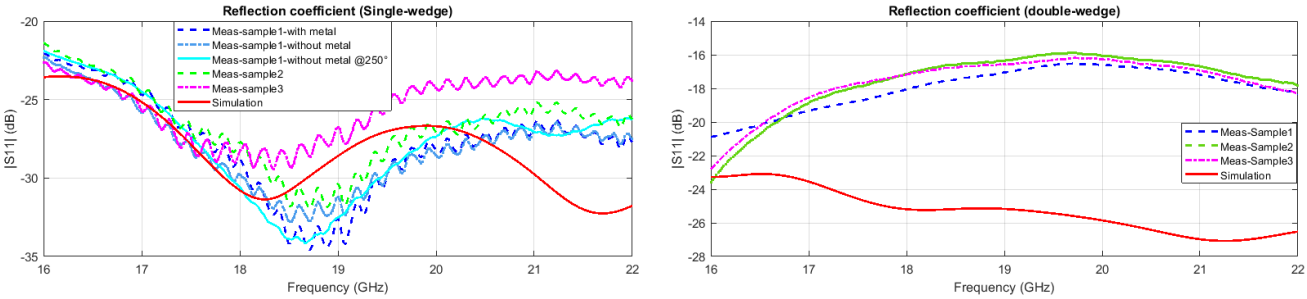
Fig. 8. Measured reflection coefficient for single- and double-wedge under power variation at 12.2 GHz

Fig. 8 summarizes the evolution of the reflection coefficient of the single- and double-linear wedge loads as the incident power is increased from 0 to 5 W. For both topologies, the reflection coefficient remains relatively stable over the entire power range with a variation of about -3.5 dB for the single-wedge and -2.5 dB for the double-wedge. Overall, both loads maintain a reflection coefficient better than approximately −16 dB over the entire power range, demonstrating good electromagnetic stability under high-temperature vacuum conditions up to an incident power of 5 W. No sudden drop or loss of matching is seen during the test. However, these tests caused slight surface degradation of the loads, with the appearance of a blister at the point of highest EM wave concentration. This degradation indicates that the components' maximum power handling capability has been exceeded under these extreme conditions of temperature and power at low pressure. Nevertheless, despite this degradation, both components retained a reflection coefficient of less than -15 dB across the frequency band of interest at the end of these tests.

KA-BAND WAVEGUIDE LOADS

Based on the Ku-band topology study, the single- and double-linear E-plane wedge loads were selected for redesign in the Ka-band (17.3–21.2 GHz). The loads were designed for a standard WR51 waveguide (12.954 mm × 6.477 mm) using PEEK-ESD as the absorbing material. The lengths of both topologies were optimized to achieve a simulated reflection coefficient below −25 dB over the entire operating frequency band. As a result, both waveguide loads have a length of 20 mm and exhibit simulated reflection coefficients lower than −25 dB across the Ka-band.

Both waveguide loads were fabricated by FDM using PEEK-ESD to evaluate their microwave performance. As shown in Fig. 9(a), excellent agreement is obtained between the simulated and measured reflection coefficients of the single-linear wedge, both with and without the metallic short-circuit plate. In all cases, the measured reflection coefficient remains below −20 dB over the entire operating frequency band. In contrast, a significant discrepancy is observed between the simulated and measured results for the double-linear wedge (Fig. 9(b)). This difference is attributed to the small dimensions of the load, which make this topology more difficult to manufacture accurately. Consequently, the single-linear wedge was selected for the Ka-band experimental tests under space-like environmental conditions.



(a) (b)

Fig. 9. Simulated and measured reflection coefficients of the (a) single-linear wedge and (b) double-linear wedge

Experimental validation in a space-like environment: vacuum and thermal testing

High-power tests under representative space environmental conditions were conducted on the single linear wedge in the Ka-band, following the same temperature test procedure used for the Ku-band measurements. As shown in Fig. 10, the reflection coefficient remains below −20 dB across the entire operating band, regardless of the temperature condition.

No significant variation in the $|S_{11}|$ level was observed, demonstrating the stability of the absorption performance over the tested temperature range

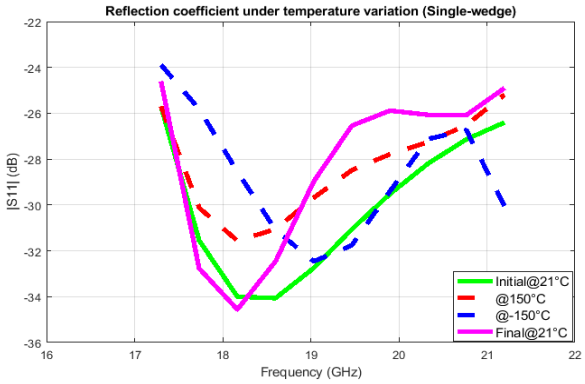


Fig. 10. Measured reflection coefficient for single linear wedges under temperature variation

High power tests were also performed on these loads at 19.25 GHz and under the same conditions than previously for Ku-band components (pressure below 5×10^{-5} mbar and ambient temperature of +150°C). The incident power was limited to 1.25 W, corresponding to the requirement of the application. Fig. 10 summarizes the evolution of the reflection coefficient of the single wedge loads as the incident power is increased from 0.25 to 1.25 W. The reflection coefficient remains stable over the entire power range with a variation of only 0.6 dB. In addition, good performance stability was demonstrated, with similar frequency responses before and after high-temperature vacuum power testing. To our knowledge, this work represents the first demonstration of the compatibility of 3D-printed absorbers with a space environment, provided that irreversibility thresholds are not exceeded.

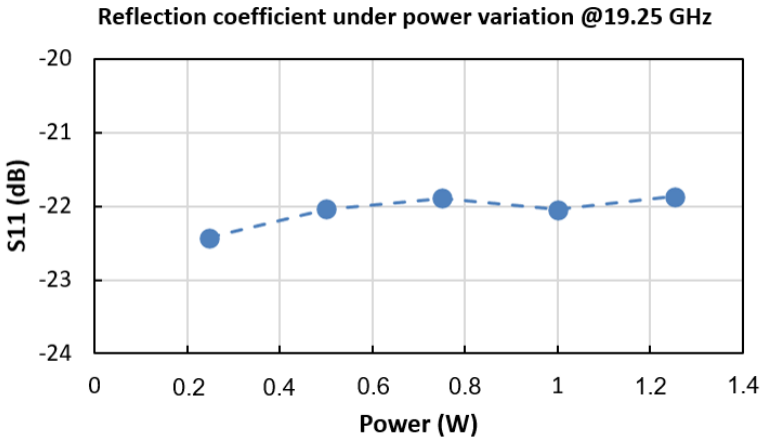


Fig. 11. Measured reflection coefficient for the single wedge under power variation at 19.25 GHz

CONCLUSION

In this work, the potential of high-temperature thermoplastic composites for the development of space-compatible rectangular waveguide loads has been investigated. The combination of advanced composite materials and 3D-printing technology provides new opportunities to optimize the trade-off between compactness, electromagnetic performance, and power-handling capability.

Among the materials investigated, the PEEK-ESD-based loads demonstrated promising performance for space applications in both the Ku- and Ka-bands. The experimental results showed good agreement with the simulations, confirming the accuracy of the design approach and the reproducibility of the manufacturing process. The double-wedge topology exhibited a higher power-handling capability than the single-wedge configuration, highlighting the advantages of topology optimization enabled by additive manufacturing.

Environmental tests performed under representative space conditions demonstrated that the proposed 3D-printed loads maintain stable electromagnetic performance under vacuum and thermal cycling conditions but also highlighted the power limitations of the load. The extension of the approach to Ka-band operation further confirmed its versatility. In

particular, the single-wedge topology maintained a reflection coefficient level below -20 dB during high-temperature vacuum power testing, with limited variation in the reflection coefficient and no significant performance degradation after testing.

Future work will focus on further enhancing the thermal management and power-handling capability of these components through additional material optimization and absorber topology refinement.

REFERENCES

[1] D.-Y. Luo, J. Deng, and R.-F. Jao, "Quantitative Analysis of a Lossy Rectangular Waveguide with Embedded High-Power Dielectric Window," in *2025 5th International Conference on Communication Technology and Information Technology (ICCTIT)*, Guangzhou, China: IEEE, Dec. 2025, pp. 389–392.

[2] P. K. Verma and R. Kumar, "Realization of Wide Band Waveguide Terminations at KuBand," *Int. J. Adv. Microw. Technol.*, vol. 3, no. 4, pp. 176–179, 2018.

[3] Y. Arbaoui *et al.*, "Full 3-D Printed Microwave Termination: A Simple and Low-Cost Solution," *IEEE Trans. Microw. Theory Tech.*, vol. 64, no. 1, pp. 271–278, Jan. 2016.

[4] H. M. Fahad, H. Huang, R. T. Mushtaq, and K. A. Al-Ghamdi, "Additively manufactured lightweight coaxial to circular waveguide transition for linearly polarized microwave systems," *Sci. Rep.*, vol. 15, no. 1, p. 27185, Jul. 2025.

[5] I. O. Saracho-Pantoja, J. R. Montejo-Garai, J. A. Ruiz-Cruz, and J. M. Rebollar, "Additive Manufacturing of 3D Printed Microwave Passive Components," in *Emerging Microwave Technologies in Industrial, Agricultural, Medical and Food Processing*, K. Y. You, Ed., InTech, 2018.

[6] A. Maalouf, R. Gingat, and V. Laur, "Additive technology applied to the realization of K-band microwave terminations: reproducibility improvement," *Cambridge University Press*, vol. 10, no. 1, pp. 3–8, Apr. 30, 2018.

[7] G. Zinkiewicz, A. Chevalier, P. Laurent, J. Benedicto, A. Maalouf, and V. Laur, "Toward Ultracompact Multi-Materials Rectangular Waveguide Terminations," *IEEE Trans. Microw. Theory Tech.*, vol. 71, no. 1, pp. 12–21, Jan. 2023.

[8] M. Rinaldi, F. Cecchini, L. Pigliaru, T. Ghidini, F. Lumaca, and F. Nanni, "Additive Manufacturing of Polyether Ether Ketone (PEEK) for Space Applications: A Nanosat Polymeric Structure," *Polymers*, vol. 13, no. 1, p. 11, Dec. 2020.

[9] I. Gibson, D. Rosen, and B. Stucker, *Additive Manufacturing Technologies*. New York: Springer, 2015.

[10] Y. Arbaoui, A. Chevalier, J. Ville, P. Queffelec, and V. Laur, "Fused deposition modeling: A new technology for the fabrication," *Space Passive Compon. Days*, 2018.

[11] A. Goulas *et al.*, "The Impact of 3D Printing Process Parameters on the Dielectric Properties of High Permittivity Composites," *Designs*, vol. 3, no. 4, p. 50, Nov. 2019.

[12] A. M. Nicolson and G. F. Ross, "Measurement of the Intrinsic Properties of Materials by Time-Domain Techniques," *IEEE Trans. Instrum. Meas.*, vol. 19, no. 4, pp. 377–382, Nov. 1970.

[13] W. B. Weir, "Automatic measurement of complex dielectric constant and permeability at microwave frequencies," *Proc. IEEE*, vol. 62, no. 1, pp. 33–36, 1974.